Nonlinear saturation of toroidal Alfven eigenmode by self-organized zonal fields in DIII-D experiments

Jian Bao

Institute of Physics, Chinese Academy of Sciences

In collaboration with Zhiyong Qiu, Zhihong Lin and Liu Chen

The 16th International West Lake Symposium on the "Physics of Fusion and Space Plasmas"

Hangzhou China 2026.4.10-4.12

Outlines

1. Background and motivation
2. TAE beat-driven zonal fields and phase space zonal structure
3. Zonal field impacts on TAE saturation for strong EP-drive case
4. Summary

Turbulence suppression by TAE: experimental evidence

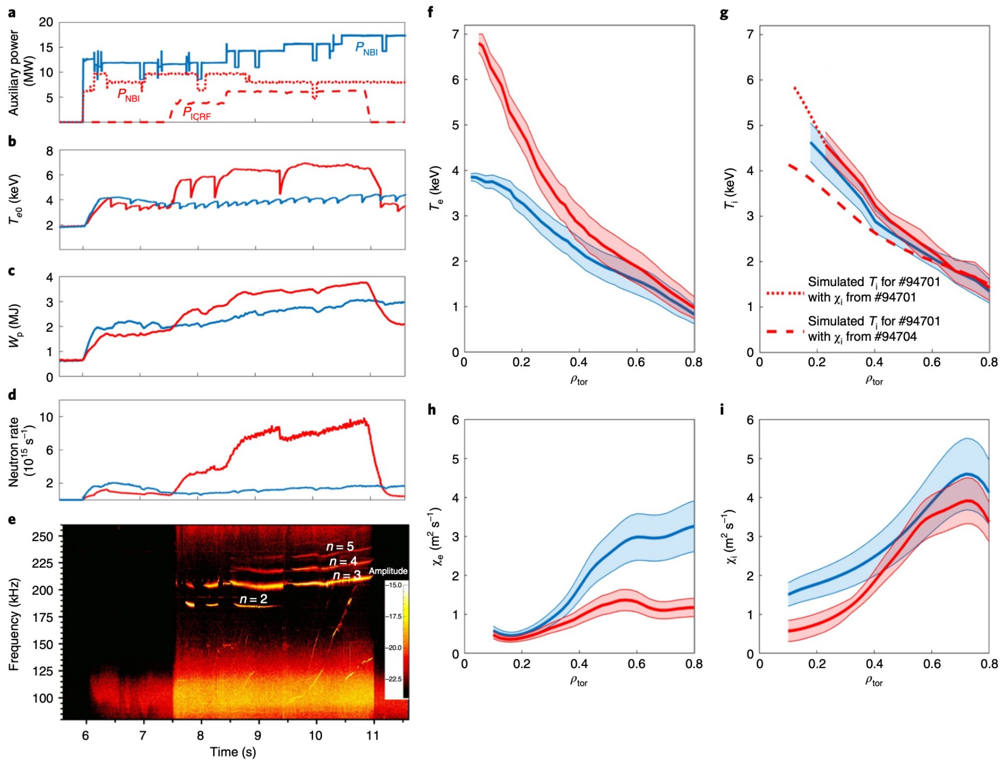

JET experiments

Mazzi S et al, Nature Physics 18, 776 (2022)

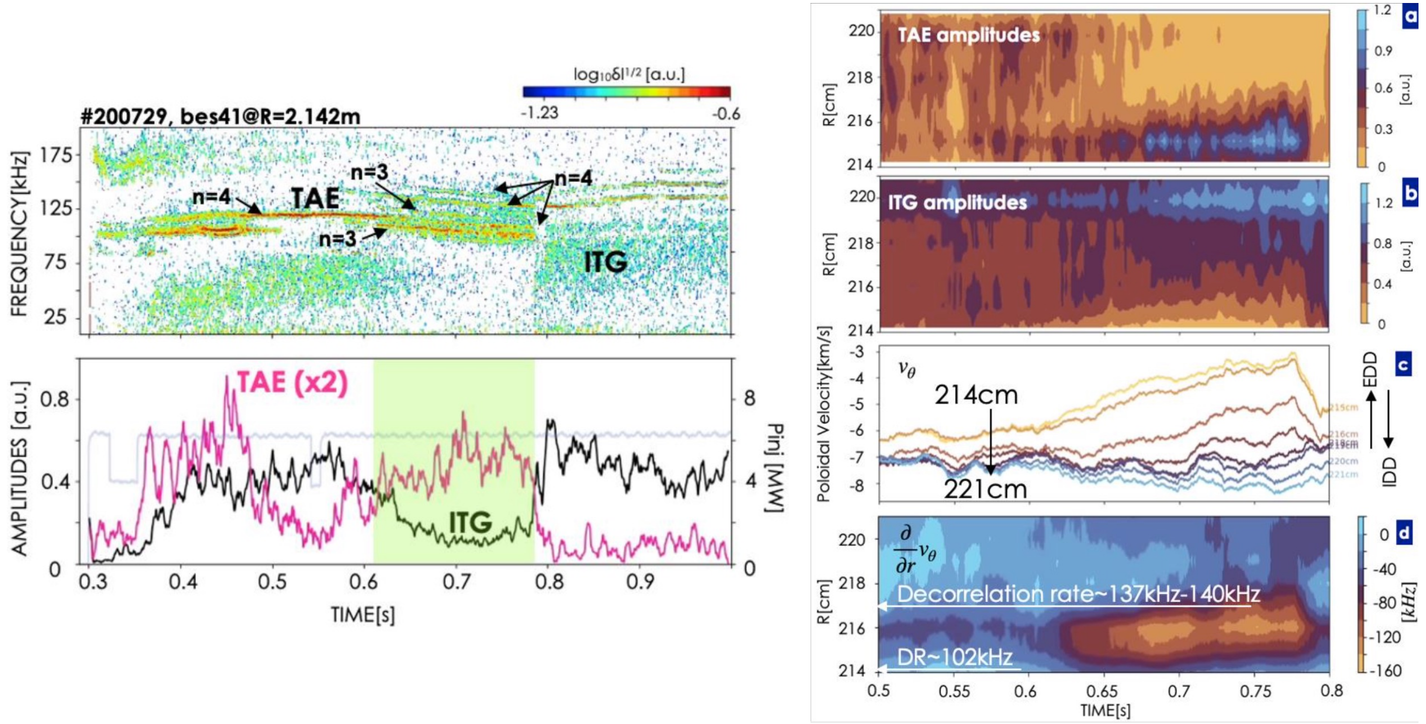

DIII-D experiments

Du X and Heidbrink W, ITPA-EP 2025

- Plasma confinement is greatly improved in presence of TAEs driven by Mev-range ions in JET tokamak.
- Recent DIII-D experiments identify the low-k ITG turbulence suppression in presence of multiple TAEs, with extensive evidence on axisymmetric shear flow layer correlated to turbulence suppression.

DIII-D experimental results of strongly unstable AEs

Left: Tobias 2011 PRL
Right: Wang 2013 PRL

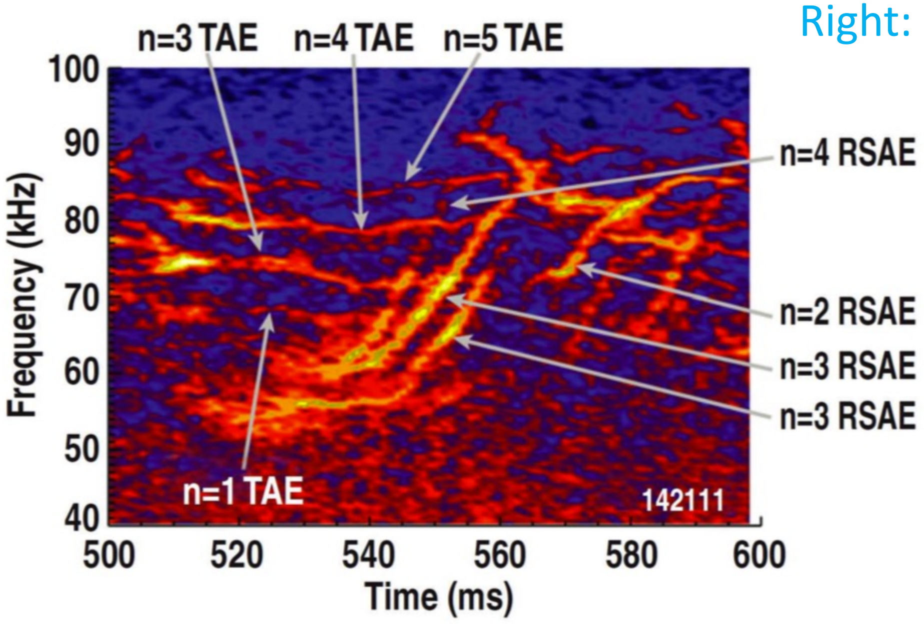

Figure: Experimental result of toroidicity induced Alfvén eigenmodes observed in DIII-D shot 142111 near 520 ms [B.J.Tobias *etc.* Phys. Review Letters **106**, 075003, (2011)]

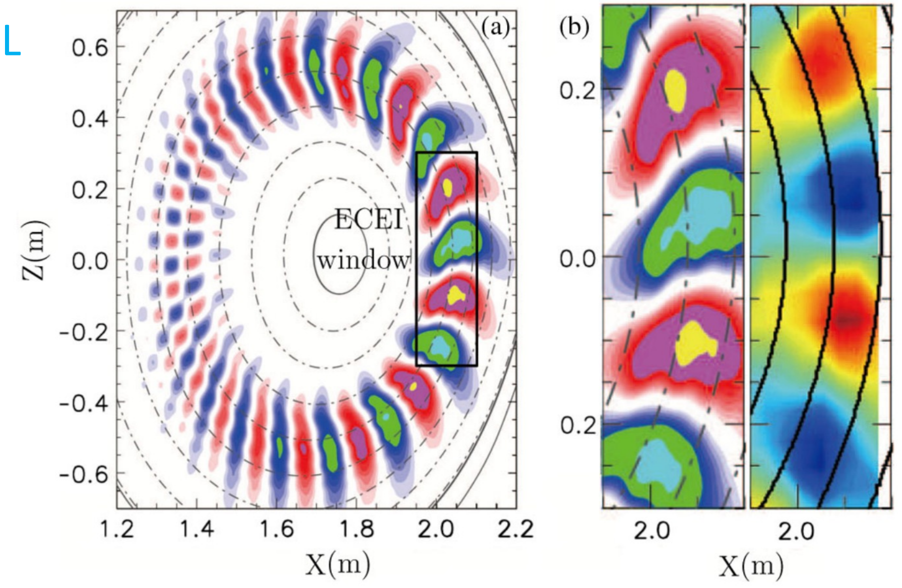

FIG. 4 (color online). (a) Contour plot of relative electron temperature perturbation $\delta T_e/T_e$ eigenstructure on a poloidal plane from GTC simulation. (b) Comparison of $\delta T_e/T_e$ structure from the simulation (left) and from the DIII-D experiment (right) in the ECEI window [the boxed region in (a)]. Red color represents positive perturbations and blue color represents negative perturbations.

- TAEs are excited by energetic particles before 528ms in DIII-D discharge #142111.
- The frequencies of TAEs are less sensitive to q than RSAE frequencies.
- GTC simulation of linear n=4 TAE mode structure (radial localization) agrees well with ECEI measurement.

Outlines

1. Background and motivation
2. TAE beat-driven zonal fields and phase space zonal structure
3. Zonal field impacts on TAE saturation for strong EP-drive case
4. Summary

Time evolution of n=4 TAE with zonal fields

- The zonal fields (zonal flow and zonal current) are beat-driven by pump-TAE with twice linear growth rates ($\gamma_{ZF} = 2\gamma^L$ and $\gamma_{ZC} = 2\gamma^L$). Lin and Bao 2017 IAEA-FEC
- Zonal fields lead to TAE saturation. Lin and Bao 2017 IAEA-FEC

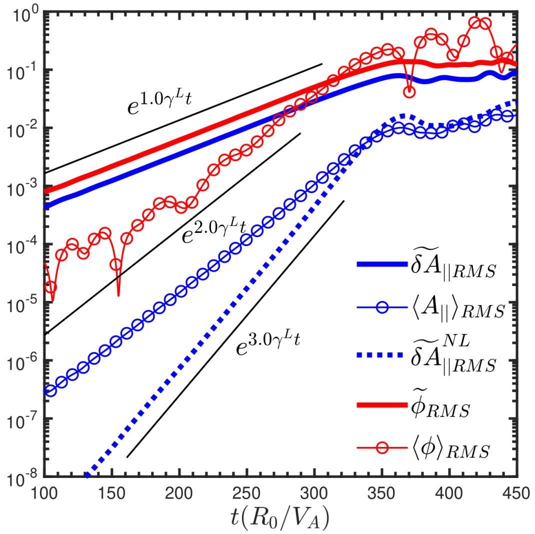

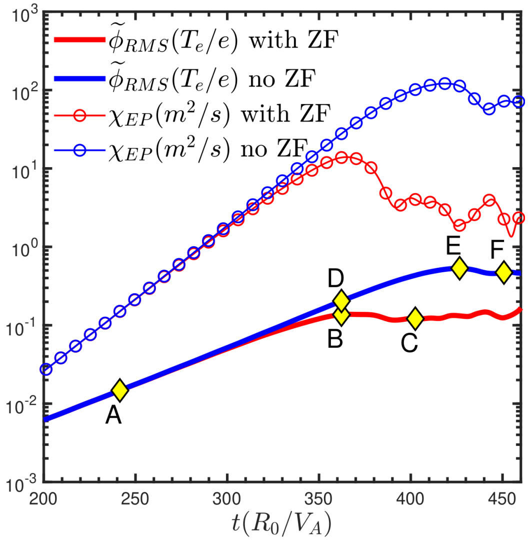

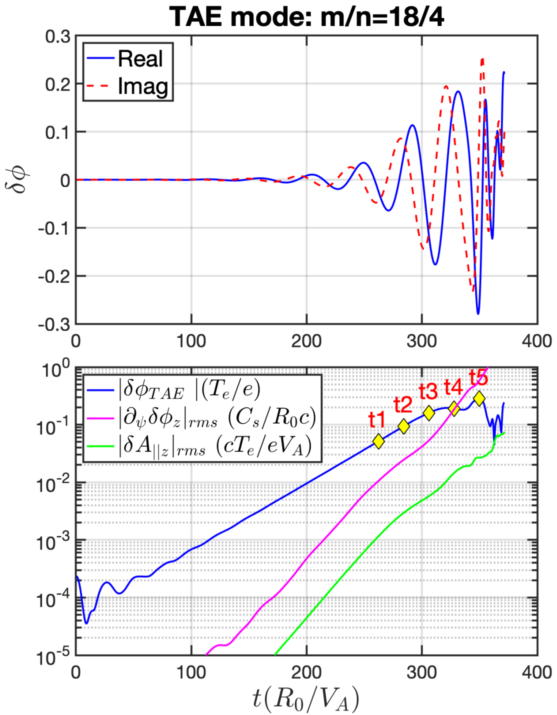

- Five snapshots, i.e., t1-t5, are chosen for detailed diagnoses which cover both linear and nonlinear saturation stages.

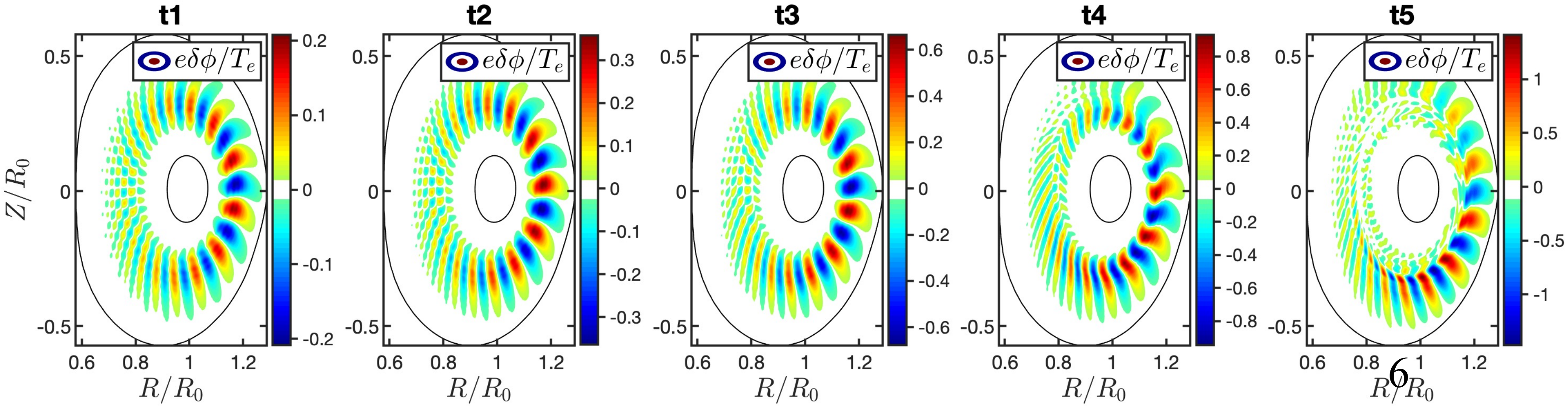

Radial structure of zonal flow and zonal current

Radial structures of zonal flow $\partial_\psi \delta\phi_z$ and zonal current $\delta A_{||z}$ at t1-t5 times.

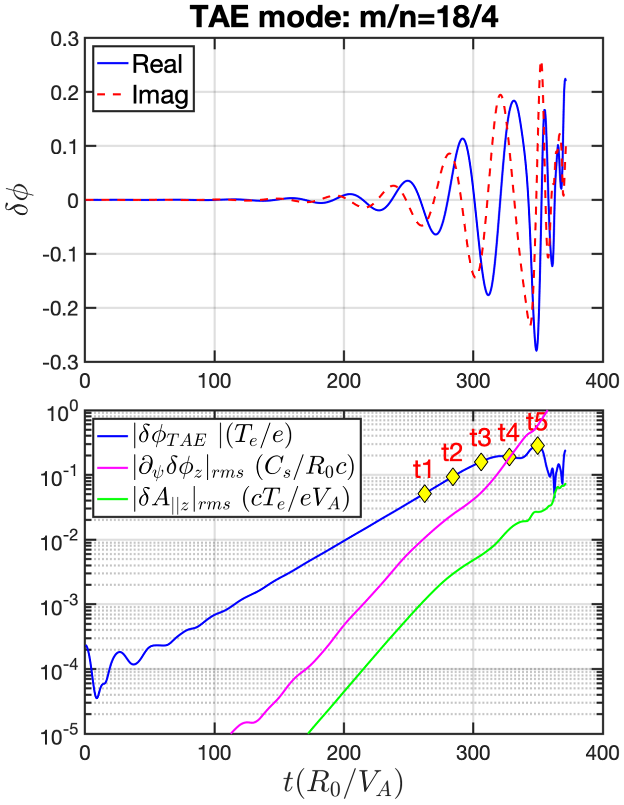

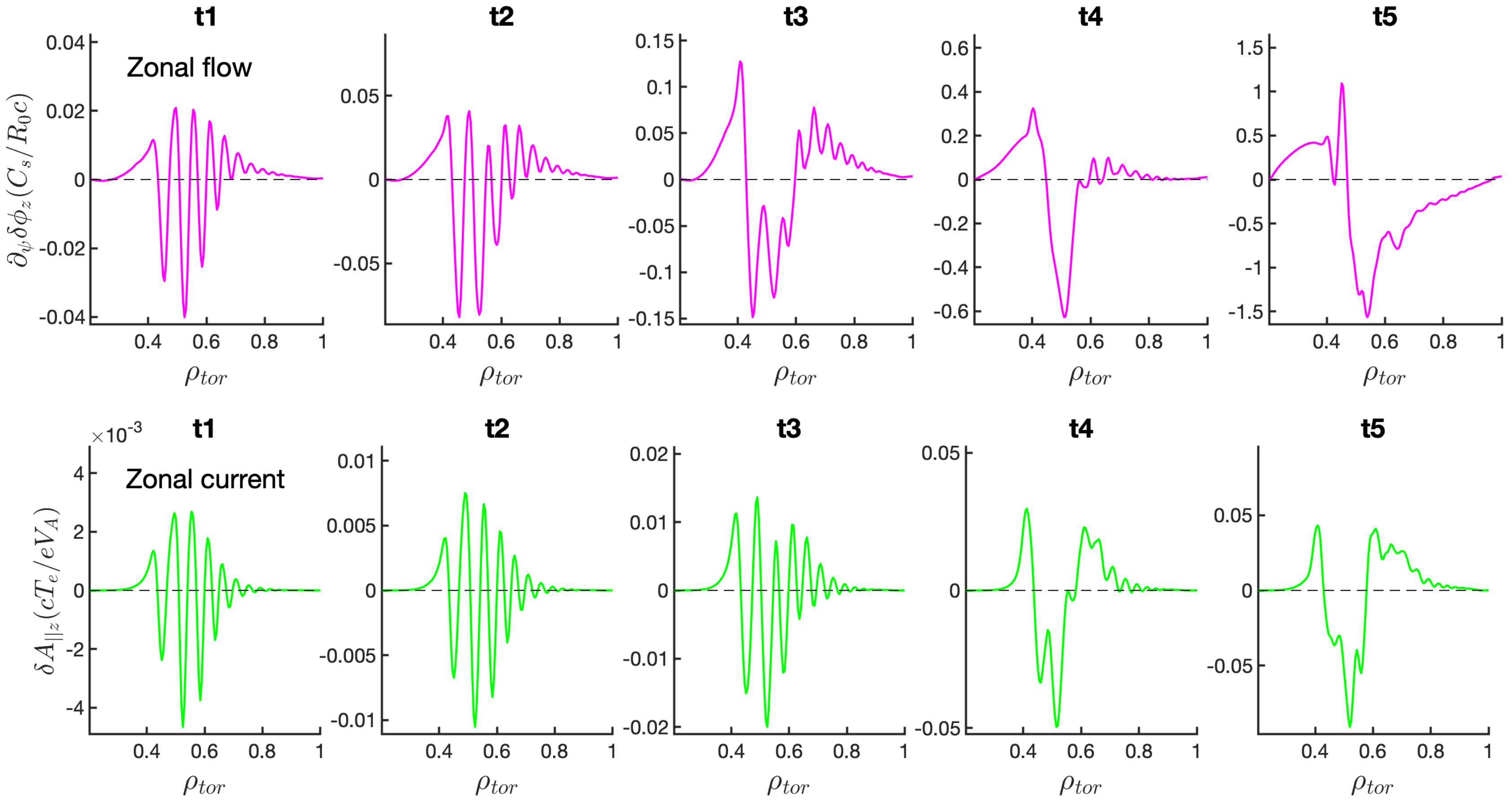

- $\partial_\psi \delta\phi_z$ and $\delta A_{||z}$ are characterized by fine radial-scale structures in linear stage.
- Consistent with gyrokinetic theory (Qiu 2016 pop, 2017NF)

Comparison of TAE beat-driven zonal current between GTC simulation and gyrokinetic theory

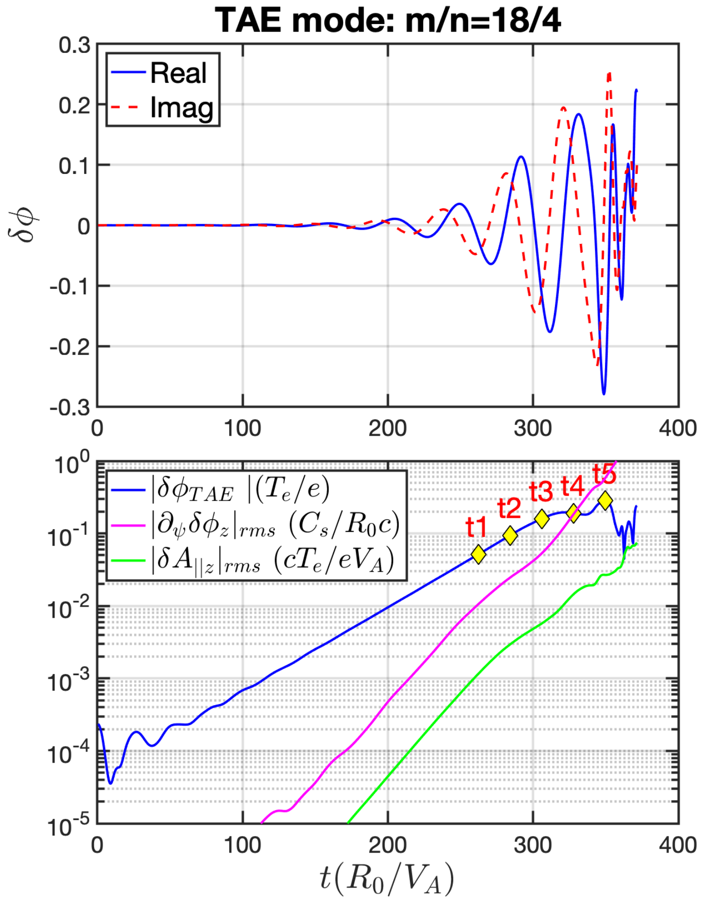

With the δg_z's derived, we can then proceed to calculate $\delta\phi_z$ and $\delta A_{\|z}$. First, the parallel Ampère's law, $\nabla_\perp^2 \delta A_{\|z} = 4\pi\delta J_z/c$, can be readily shown to yield [20]

$$\frac{A_z}{c} \simeq \frac{c}{B_0\omega_{0r}^2}\frac{\partial}{\partial r}\left[k_{\theta 0}k_{\|0}|\delta\psi_0|^2\right] \simeq \frac{c}{B_0\omega_{0r}^2}\frac{\partial}{\partial r}\sum_m\left(\frac{n_0 q}{r}\right)\frac{(n_0 q - m)}{qR}|\Phi_m|^2. \qquad (29)$$

Chen et al, Nucl. Fusion 2025

Extension in flux coordinate for general geometry

$$\delta A_{\|z} = \frac{nc^2}{JB_0^2}\frac{1}{\omega_{0r}^2}\sum_m \frac{\partial}{\partial\psi}\widetilde{B}_{0,0}|\widetilde{\delta\psi}_m|^2(nq-m)$$

Bao, Qiu, Chen 2026

t=t1 stage

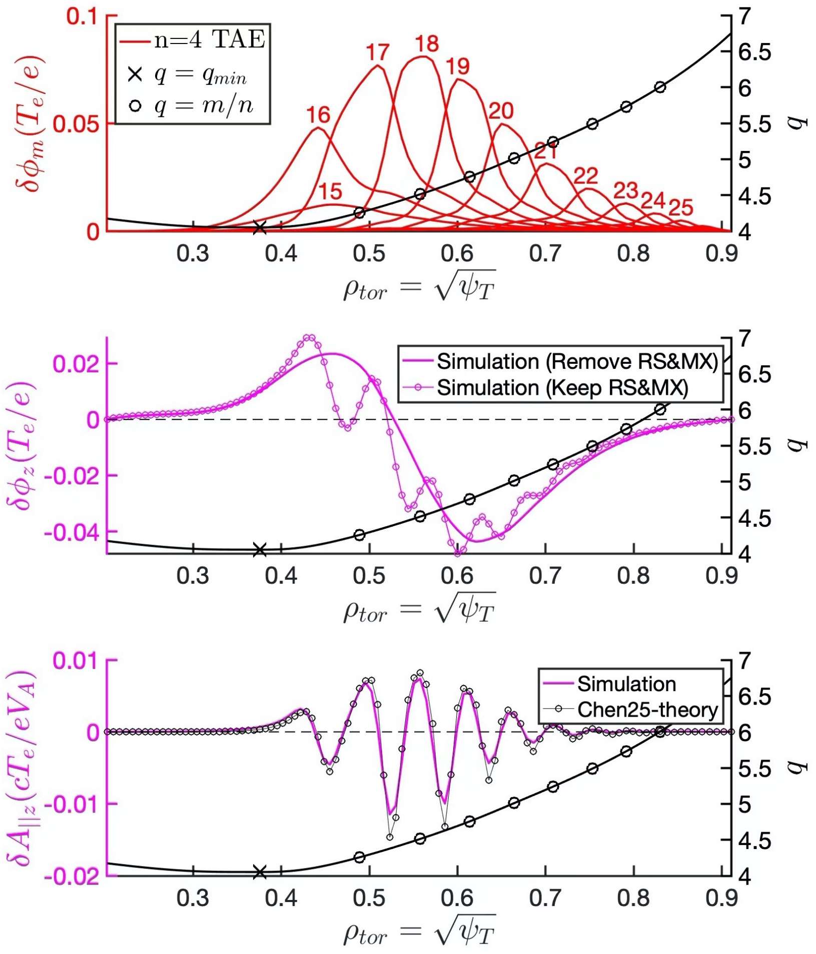

- Simulation and theory shows excellent agreement on beat-driven ZC!

Zonal current modification on q profile (single n=4 TAE)

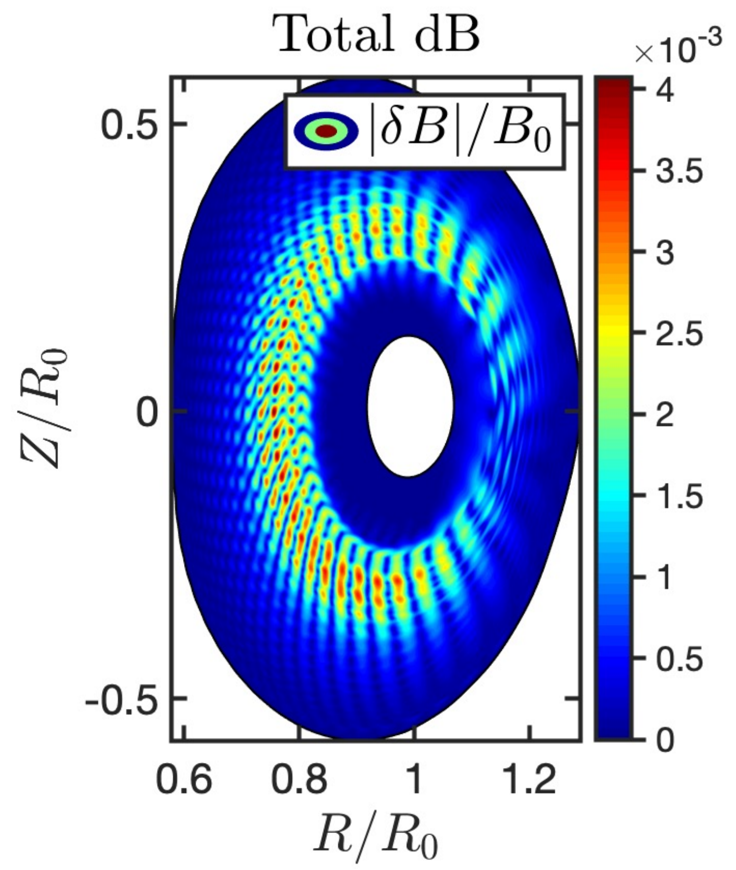

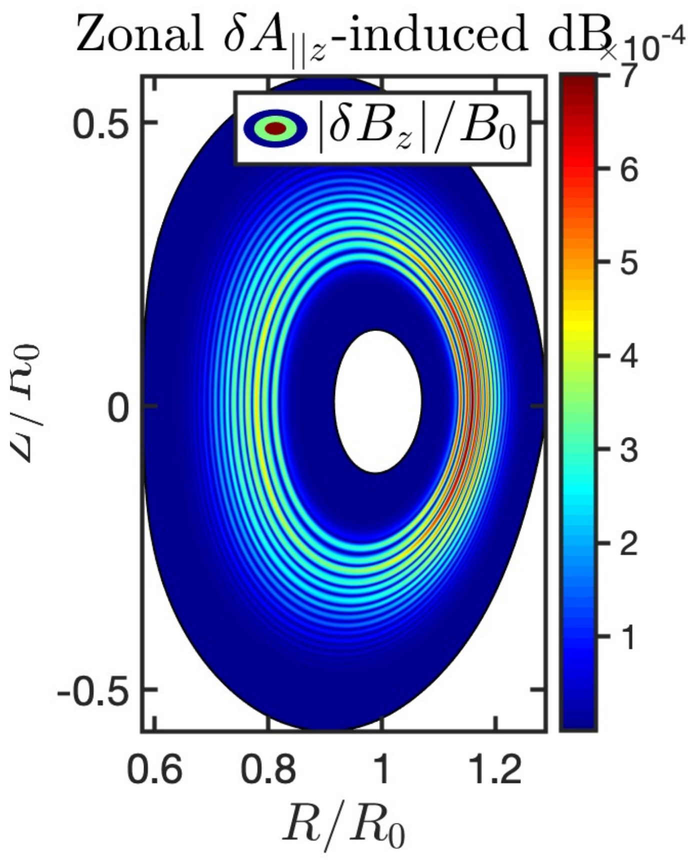

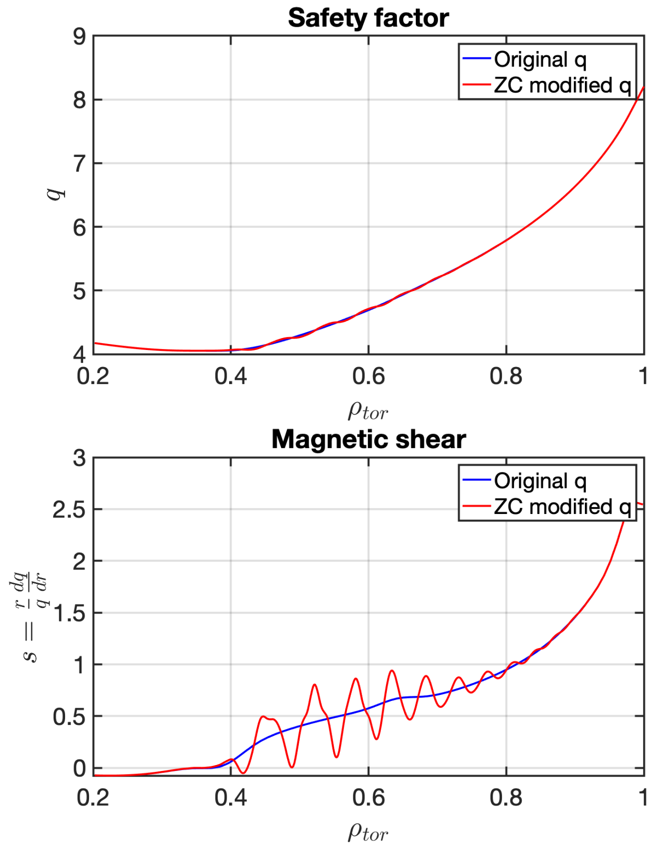

- For single TAE saturation with $\frac{\delta B}{B_0} \sim 4\times 10^{-3}$ at the peak amplitude, the zonal current ($\delta A_{||z}$) contributes to the magnetic perturbation with $\frac{\delta B_z}{B_0} \sim 7\times 10^{-4}$. ($\delta B_z = \nabla \delta A_{||z} \times b_0$)
- The ratio between zonal current contribution and total magnetic perturbation is about $\frac{\delta B_z}{\delta B} \sim 0.175$.
- The zonal current from single TAE can modify the q profile with 'staircase' stucture, which leads to the oscillations on magnetic shear that might modulate high-n drift waves.

EP phase space zonal structure (PSZS) in (ρ_{tor}, E, μ) coordinates

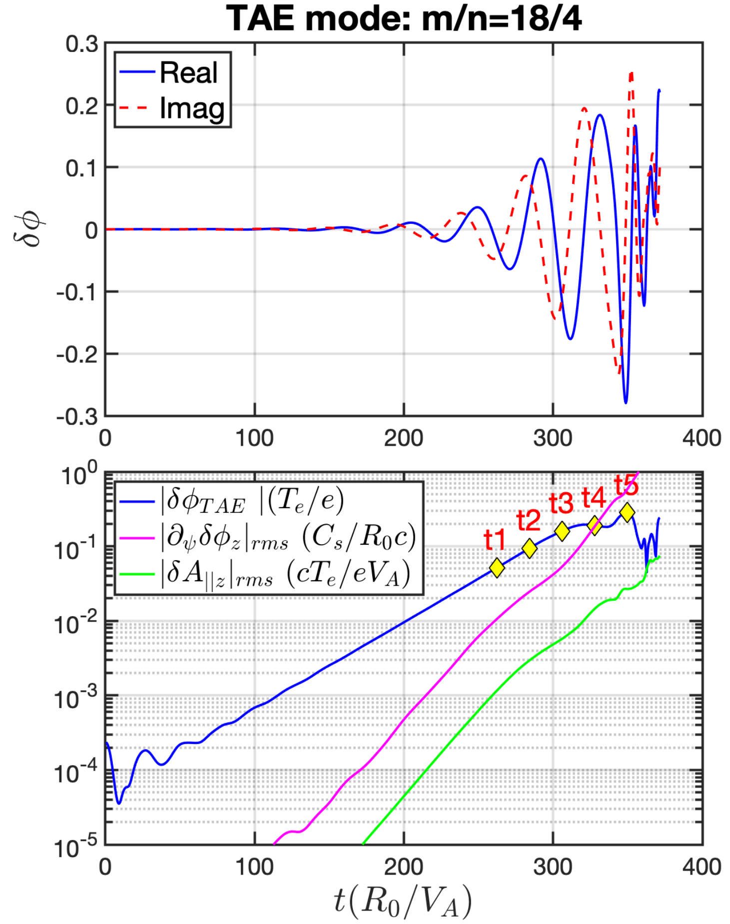

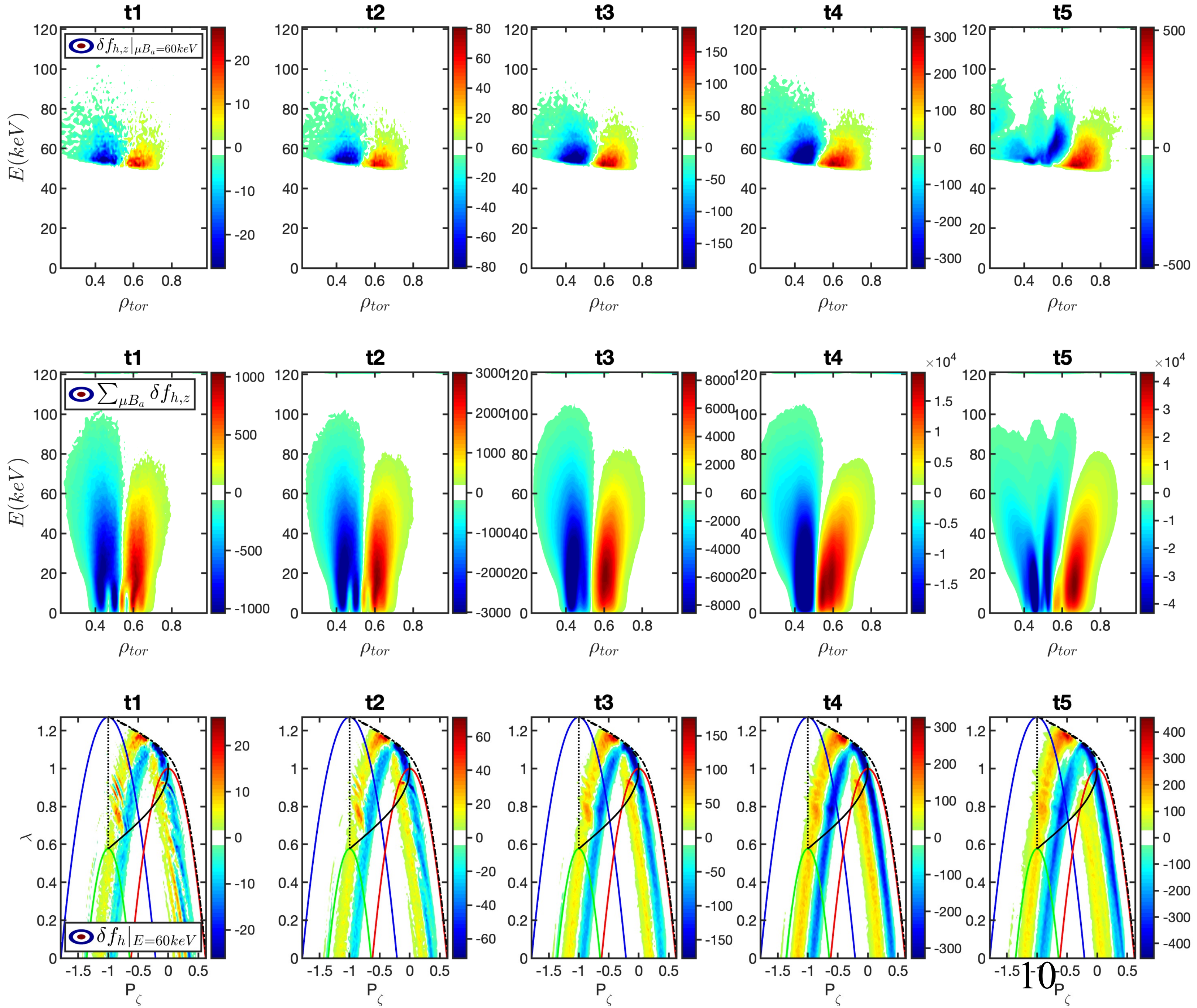

Correlation between EP-PSZS and TAE mode structure

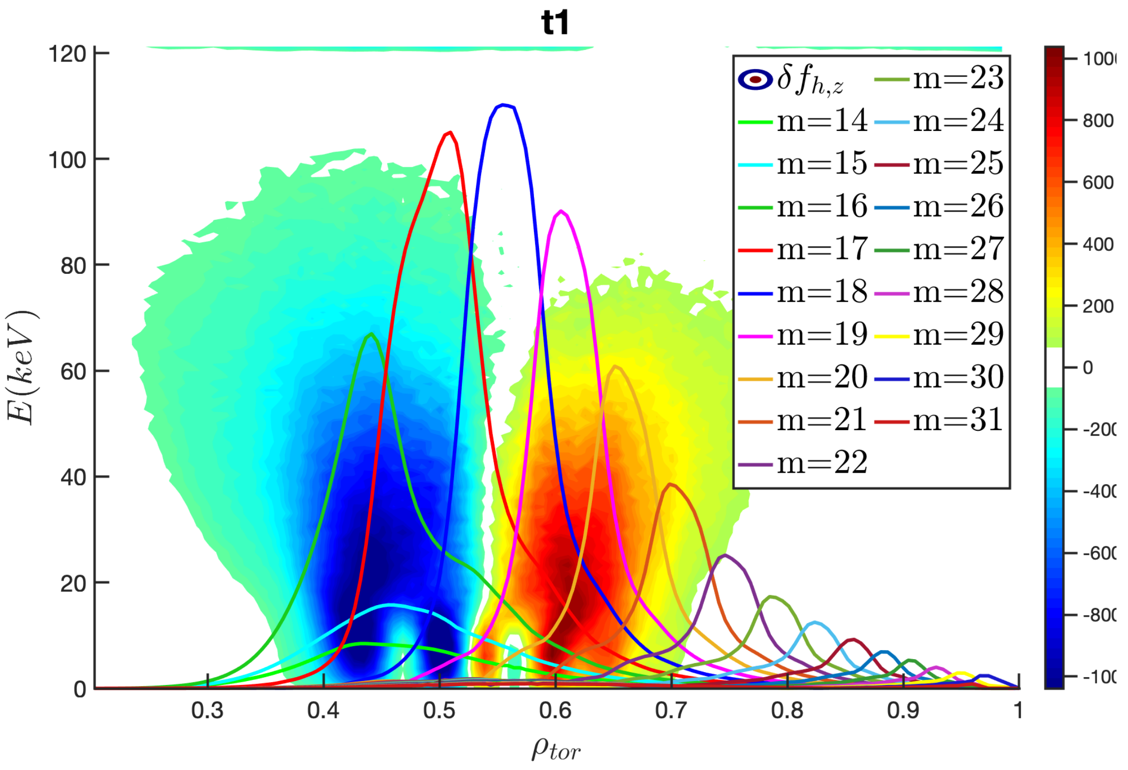

EP-PSZS

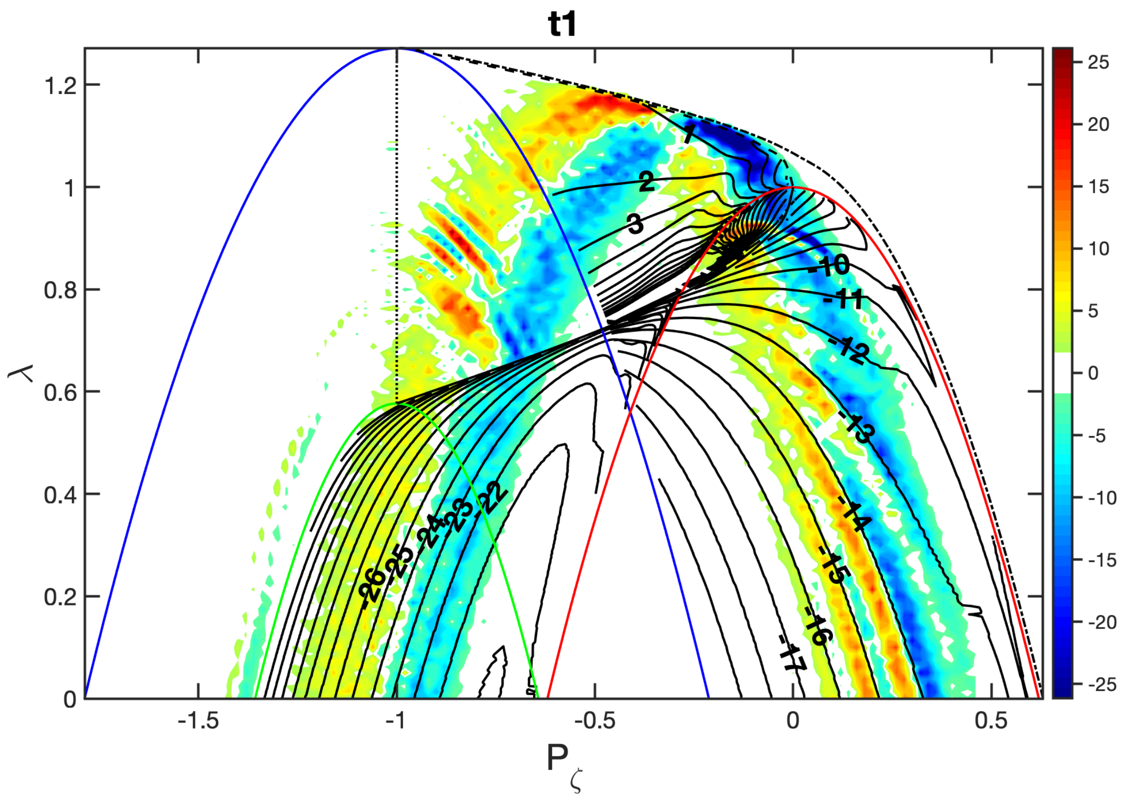

EP-TAE resonances in CoM phase space

Outlines

1. Background and motivation
2. TAE beat-driven zonal fields and phase space zonal structure
3. Zonal field impacts on TAE saturation for strong EP-drive case
4. Summary

Correlation between PSZS and zonal density/temperature

Thermal ion-PSZS $\delta f_{z,i}$ in linear stage (time=t1)

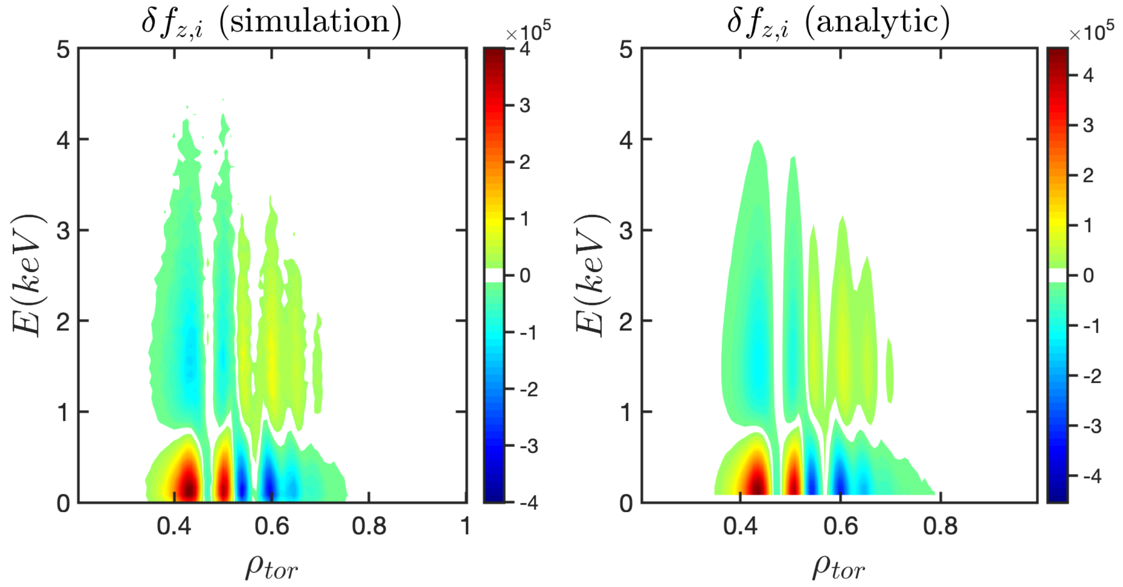

Thermal ion-PSZS $\delta f_{z,i}$ in nonlinear stage (time=t5)

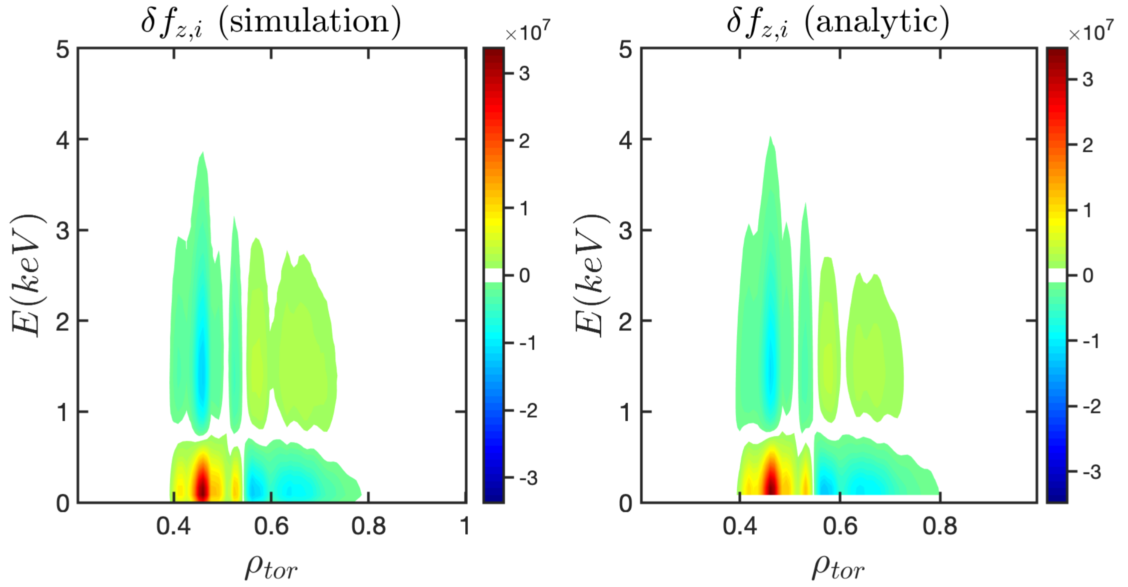

The anisotropic equilibrium distribution can be expressed as

$$f_{\alpha 0} = n_{\alpha 0}\left(\frac{m_\alpha}{2\pi T_{||\alpha 0}}\right)^{1/2}\left(\frac{m_\alpha}{2\pi T_{\perp\alpha 0}}\right) exp\left[-\frac{m_\alpha\left(v_{|} - u_{||0}\right)^2}{2T_{||\alpha 0}}\right] exp\left(-\frac{\mu B_0}{T_{\perp\alpha 0}}\right)$$

and the corresponding PSZS in the lowest order is

$$\delta f_z = \frac{\partial f_{\alpha 0}}{\partial n_{\alpha 0}}\delta n_z + \frac{\partial f_{\alpha 0}}{\partial T_{||\alpha 0}}\delta T_{||z} + \frac{\partial f_{\alpha 0}}{\partial T_{\perp\alpha 0}}\delta T_{\perp z} + \frac{\partial f_{\alpha 0}}{\partial u_{||\alpha 0}}\delta u_{||z}$$

$$\delta f_z = \frac{\delta n_z}{n_{\alpha 0}} f_{\alpha 0} + \frac{\delta T_{||z}}{T_{||\alpha 0}}\left[\frac{m_\alpha\left(v_{||} - u_{||\alpha 0}\right)^2}{2T_{||\alpha 0}} - \frac{1}{2}\right] f_{\alpha 0} + \frac{\delta T_{\perp z}}{T_{\perp\alpha 0}}\left(\frac{\mu B_0}{T_{\perp\alpha 0}} - 1\right) f_{\alpha 0} + \frac{m_\alpha}{T_{||\alpha 0}}\left(v_{||} - u_{||\alpha 0}\right)\delta u_{||z} f_{\alpha 0}$$

- In Maxwellian equilibrium, the analytic expression of thermal ion-PSZS $\delta f_{z,i}$ agrees well with GTC simulation in both linear and nonlinear stages.
- Therefore, $\delta f_{z,i}$ can be safely calculted using zonal density $\delta n_{z,i}$ and zonal temperature $\delta T_{z,i}$, which bring convenience for computing nonlinear diamagnetic frequency with quantitative accracy.

Nonlinear voticity equation consistent with theory

General expression of nonlinear voticity equation from Chen L and Zonca F, 2016 RMP

$$B_0\left(\nabla_{||}+\frac{\boldsymbol{\delta B_\perp}}{B_0}\cdot\boldsymbol{\nabla}\right)\left(\frac{\delta j_{||}}{B_0}\right)-\boldsymbol{\nabla}\cdot\sum\left\langle\frac{e^2}{m}\frac{2\mu}{\Omega^2}\left(B_0\frac{\partial F_0}{\partial\epsilon}+\frac{\partial F_0}{\partial\mu}\right)\left(\frac{J_0^2-1}{\lambda^2}\right)\right\rangle_v\boldsymbol{\nabla}_\perp\frac{\partial}{\partial t}\delta\phi$$

$$-\sum ec\mathbf{b_0}\times\boldsymbol{\nabla}\left\langle\frac{2\mu}{\Omega^2}F_0\left(\frac{J_0^2-1}{\lambda^2}\right)\right\rangle_v\cdot\boldsymbol{\nabla}\nabla_\perp^2\delta\phi+\frac{c}{B_0}\mathbf{b_0}\times\boldsymbol{\kappa}\cdot\boldsymbol{\nabla}\sum\left\langle m\left(\mu B_0+v_{||}^2\right)J_0\delta g\right\rangle_v$$

$$+\boldsymbol{\delta B_\perp}\cdot\boldsymbol{\nabla}\left(\frac{j_{||0}}{B_0}\right)+\underbrace{\sum e\left\langle J_0\left[\frac{c}{B_0}\mathbf{b_0}\times\boldsymbol{\nabla}\left(J_0\delta\phi\right)\cdot\boldsymbol{\nabla}\delta g\right]-\frac{c}{B_0}\mathbf{b_0}\times\boldsymbol{\nabla}\delta\phi\cdot\boldsymbol{\nabla}\left(J_0\delta g\right)\right\rangle_v}_{Key\ nonlinear\ terms}$$

$$+\frac{c}{B_0}\mathbf{b_0}\times\boldsymbol{\nabla}\delta\phi\cdot\boldsymbol{\nabla}\left[\boldsymbol{\nabla}\cdot\sum\left\langle\frac{e^2}{m}\frac{2\mu}{\Omega^2}\frac{\partial F_0}{\partial\mu}\left(\frac{1-J_0^2}{\lambda^2}\right)\right\rangle_v\boldsymbol{\nabla}_\perp\delta\phi\right]=0$$

Explicitly integrating the nonlinear diamagnetic response and reysolds stress terms using analytic $\delta f_{z,i}$ as a function of zonal density $\delta n_{z,i}$ and zonal temperature$\delta T_{z,i}$

$$\underbrace{\sum e\left\langle J_0\left[\frac{c}{B_0}\mathbf{b_0}\times\boldsymbol{\nabla}\left(J_0\delta\phi\right)\cdot\boldsymbol{\nabla}\delta g\right]-\frac{c}{B_0}\mathbf{b_0}\times\boldsymbol{\nabla}\delta\phi\cdot\boldsymbol{\nabla}\left(J_0\delta g\right)\right\rangle_v}_{Key\ nonlinear\ terms}$$

$$=\underbrace{\frac{c}{B_0}\sum e\left\langle J_0\left[\mathbf{b_0}\times\boldsymbol{\nabla}\left(J_0\delta\phi\right)\cdot\boldsymbol{\nabla}\langle e^{\rho\cdot\nabla}\delta f\rangle\right]-\mathbf{b_0}\times\boldsymbol{\nabla}\delta\phi\cdot\boldsymbol{\nabla}\langle\delta f\rangle\right\rangle_v}_{nonlinear\ diamagnetic\ response}$$

$$\underbrace{-\frac{c}{B_0}\sum e\left\langle J_0\left[\mathbf{b_0}\times\boldsymbol{\nabla}\left(J_0\delta\phi\right)\cdot\boldsymbol{\nabla}\left(\frac{e}{m}\frac{\partial F_0}{\partial\epsilon}J_0\delta\phi\right)\right]-\mathbf{b_0}\times\boldsymbol{\nabla}\delta\phi\cdot\boldsymbol{\nabla}\left(\frac{e}{m}\frac{\partial F_0}{\partial\epsilon}\delta\phi\right)\right\rangle_v}_{Reynolds\ stress}$$

$$\approx\underbrace{-i\omega_{nz,i}^*\frac{Z_i^2n_{i0}}{T_{i0}}\delta\phi\left(\Gamma_0\left(b_i\right)-1\right)-i\omega_{Tz,i}^*\frac{Z_i^2n_{i0}}{T_{i0}}\delta\phi\left(-b_i\Gamma_0\left(b_i\right)+b_i\Gamma_1\left(b_i\right)\right)}_{nonlinear\ diamagnetic\ drift}+\widetilde{\mathbf{V_E}}\cdot\nabla\left[\frac{Z_i^2n_{i0}}{T_{i0}}\delta\phi_z\left(1-\Gamma_0\left(b_{z,i}\right)\right)\right]$$

$$\underbrace{+i\omega_{Ez}\left[\frac{Z_i^2n_{i0}}{T_{i0}}\delta\phi\left(1-\Gamma_0\left(b_i\right)\right)\right]}_{zonal\ flow\ scattering}$$

$$-i\omega\frac{c}{V_A^2}\nabla_\perp^2\delta\phi+i\omega_{p,i}^*\frac{c}{V_A^2}\nabla_\perp^2\delta\phi+i\omega_{pz,i}^*\frac{c}{V_A^2}\nabla_\perp^2\delta\phi+i\omega_{Ez}\frac{c}{V_A^2}\nabla_\perp^2\delta\phi+\boldsymbol{\delta B_z}\cdot\nabla\left[\frac{1}{B_0}\left(\nabla_\perp^2\delta A_{||}\right)\right]$$

$$+\mathbf{B_0}\cdot\nabla\left[\frac{1}{B_0}\left(\nabla_\perp^2\delta A_{||}\right)\right]-\frac{4\pi}{c}\boldsymbol{\delta B}\cdot\nabla\left(\frac{J_{||0}}{B_0}\right)-8\pi\nabla\left(\delta P_i+\delta P_e\right)\cdot\frac{\mathbf{b_0}\times\boldsymbol{\kappa}}{B_0}$$

$$-4\pi\nabla\left(\delta P_{h||}^A+\delta P_{h\perp}^A\right)\cdot\frac{\mathbf{b_0}\times\boldsymbol{\kappa}}{B_0}-\frac{4\pi Z_h}{c}\langle\mathbf{v_d}\cdot\nabla\delta K_h\rangle_v=0$$

$$\omega_{nz,i}^*=\frac{cT_{i0}\mathbf{k}\times\mathbf{b_0}}{Z_in_{i0}B_0}\cdot\nabla\delta n_{z,i}=-\frac{cT_{i0}}{Z_in_{i0}}n\frac{\partial\delta n_{z,i}}{\partial\psi}$$

$$\omega_{Tz,i}^*=\frac{c\mathbf{k}\times\mathbf{b_0}}{Z_iB_0}\cdot\nabla\delta T_{z,i}=-\frac{c}{Z_i}n\frac{\partial\delta T_{z,i}}{\partial\psi}$$

$$\omega_{Ez}=\mathbf{k}\cdot\frac{c\mathbf{b_0}\times\nabla\delta\phi_z}{B_0}=-cn\frac{\partial\delta\phi_z}{\partial\psi}$$

- The blue terms represents nonlinear diamagnetic response and zonal flow Dopper-shift effects, which influence both TAE and continuum.

The nonlinear frequencies of $\omega_{E,z}$ and $\omega^{*}_{p,z}$ (norm by ω_{TAE})

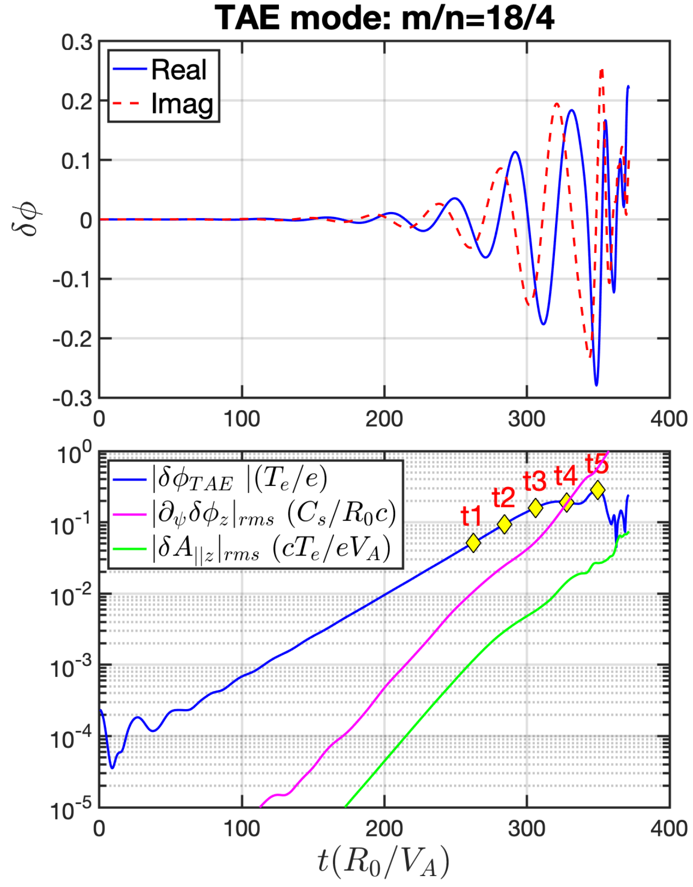

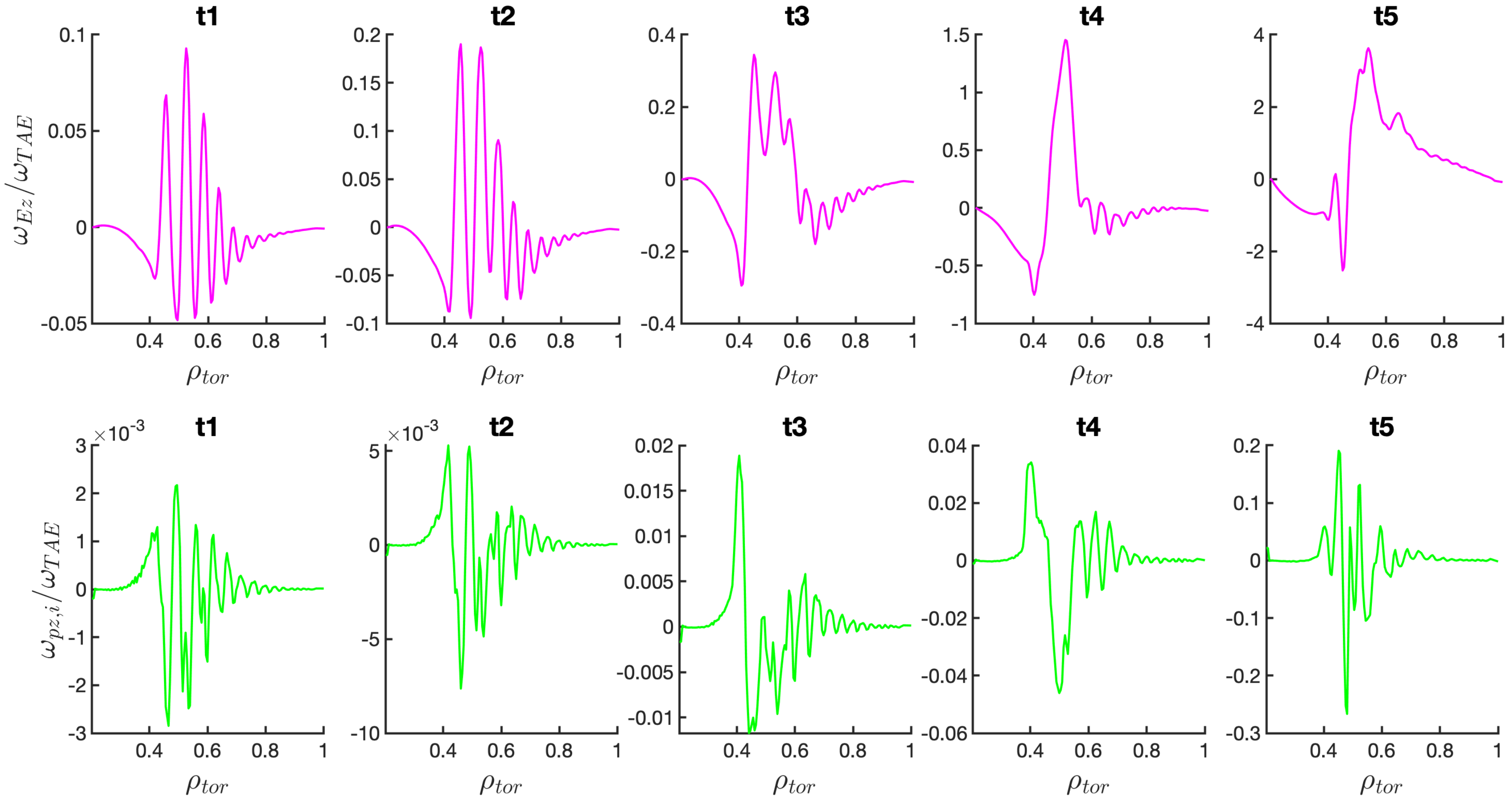

- For strong EP-drive case, the zonal flow-induced Doppler shift $\omega_{E,z}$ can be comparable to linear TAE frequency ω^{L}_{TAE} in the nonlinear saturation beginning (t3 time) , the nonlinear diamganetic frequency $\omega^{*}_{pz,i}$ is one order of magnitude smaller than $\omega_{E,z}$.

Nonlinear frequency modification on continuum

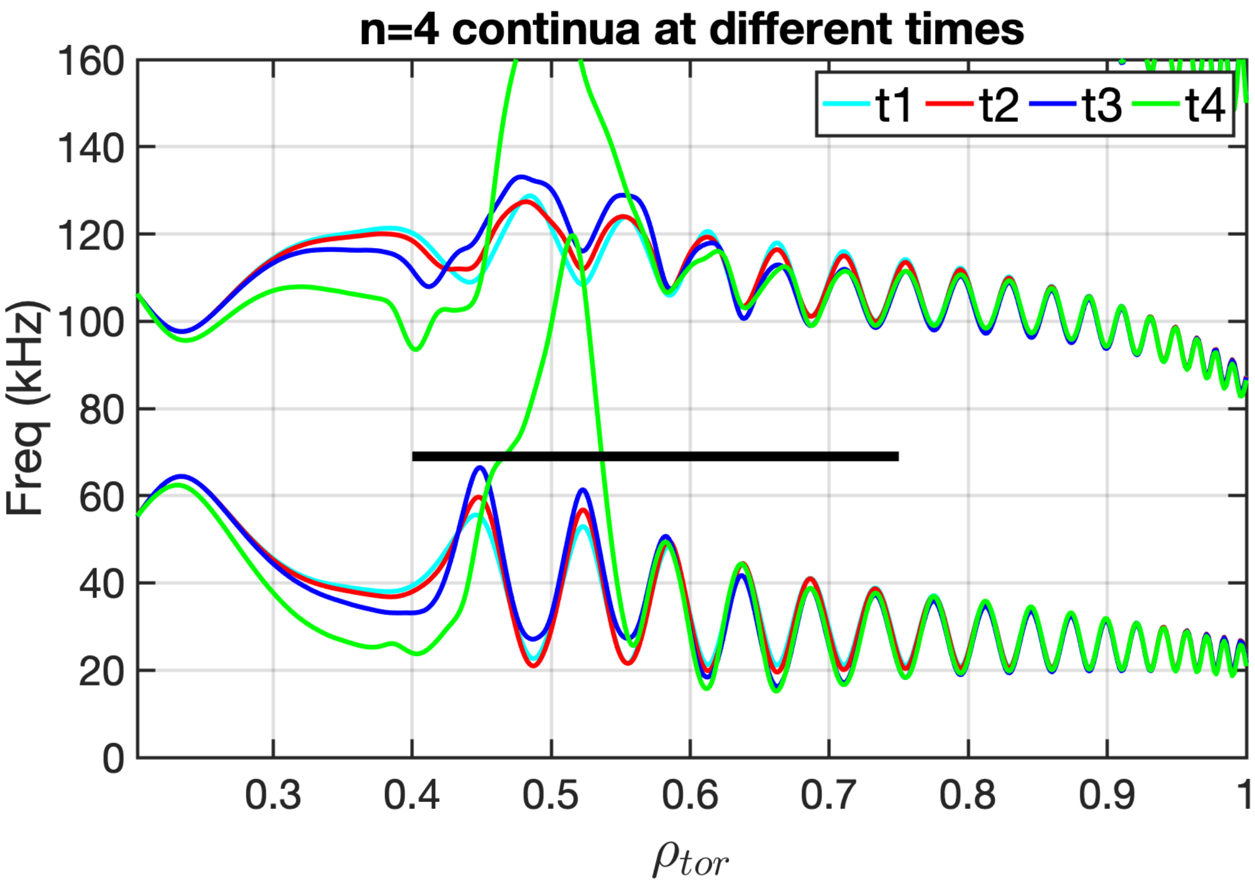

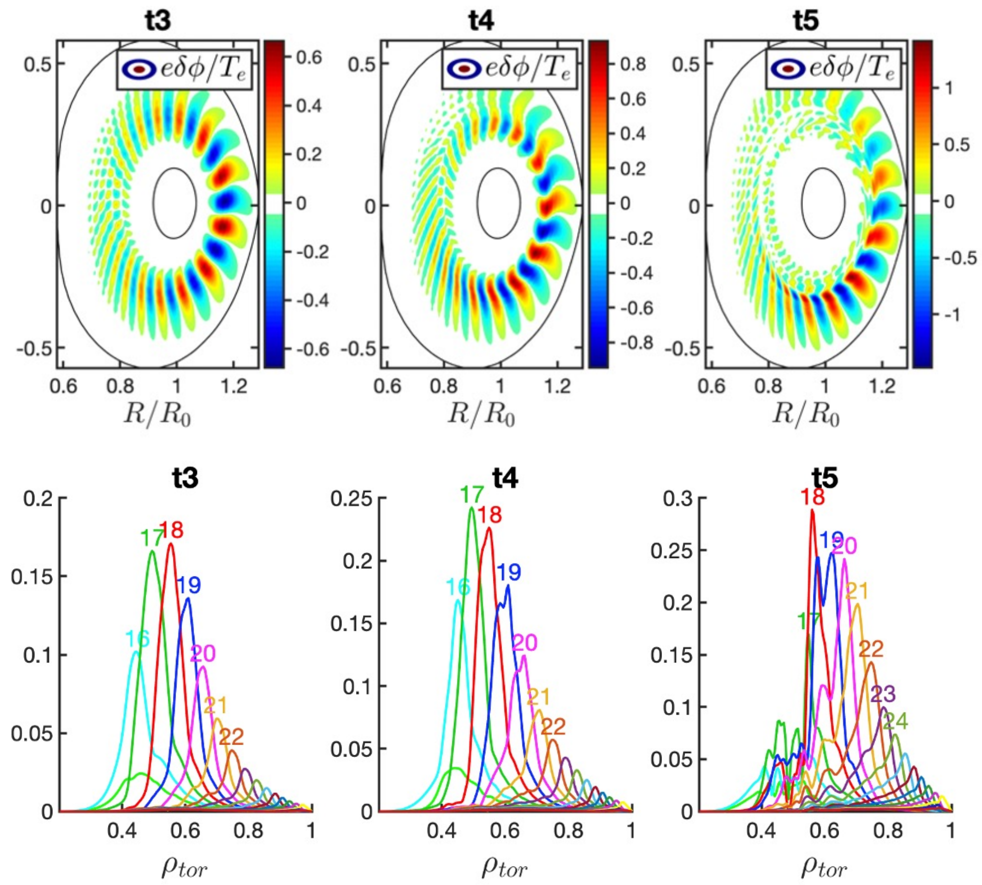

- The Alfven continua fast move to TAE and lead to strong continuum damping, consistent to the radial damping location on TAE mode structure. (there is a time delay related to phase-mixing time)

Each zonal component contribution

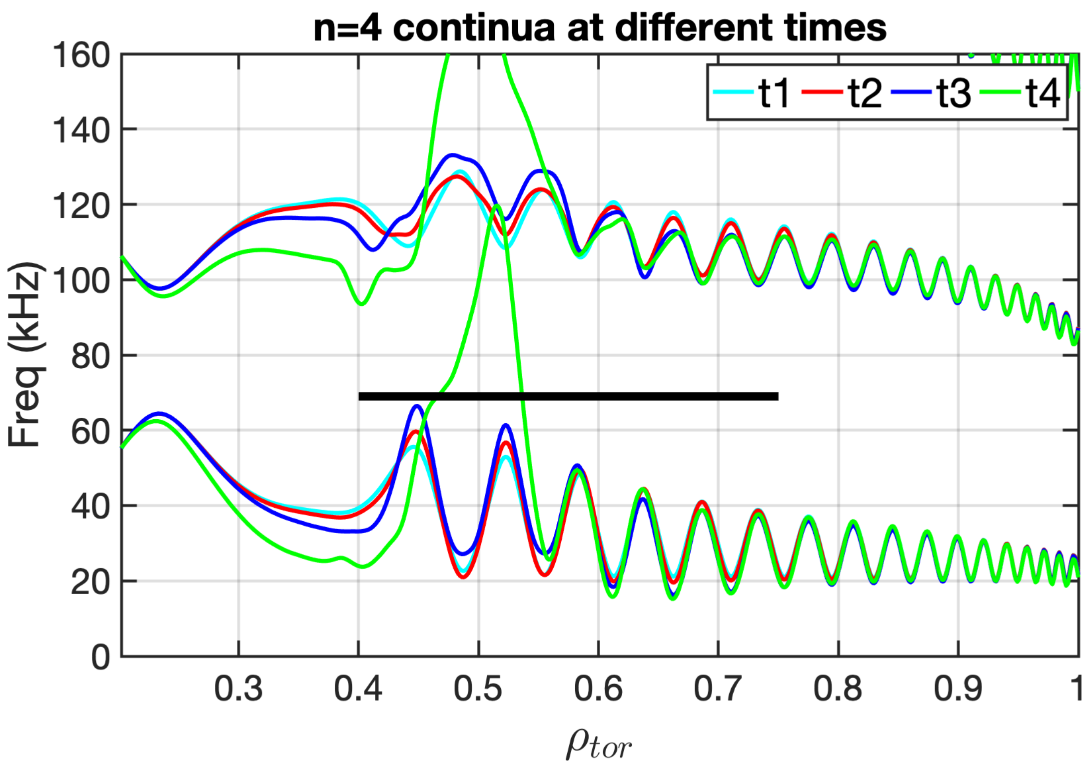

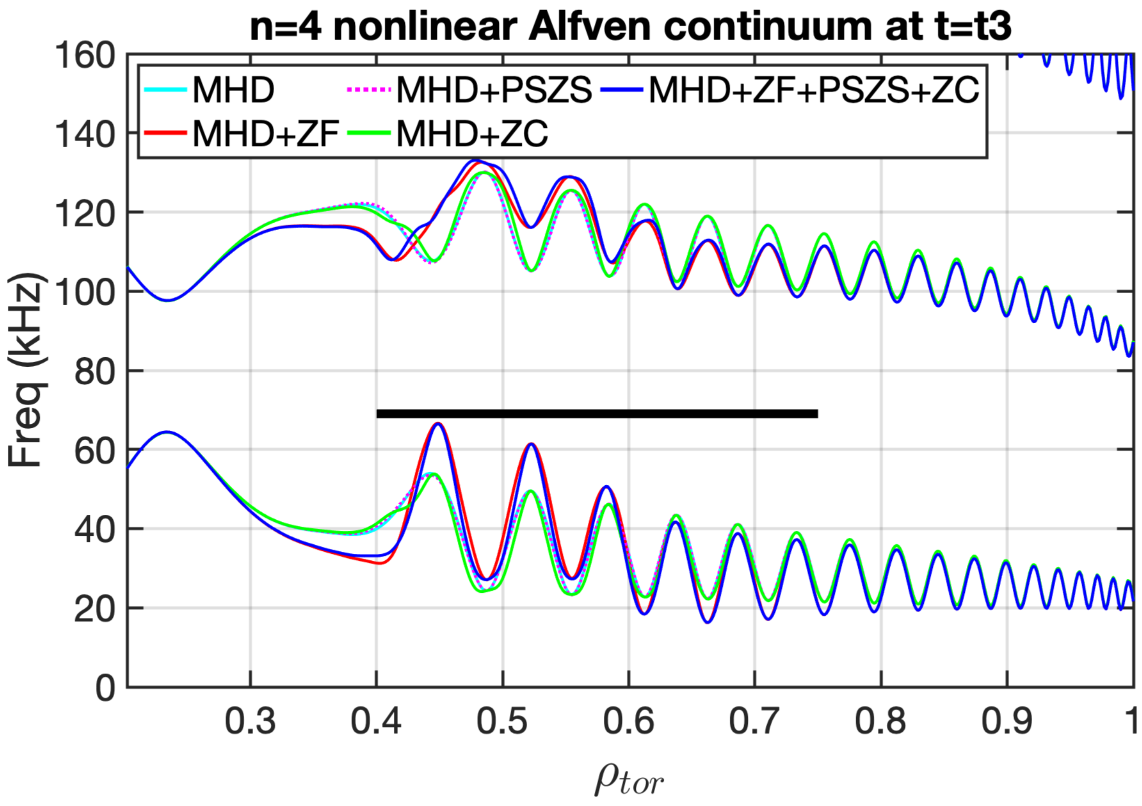

- For strong EP-drive case, zonal flow dominates over zonal current and PSZS on continuum modification.
- In fution reactor regime such as ITER-baseline scenario, AEs are maginal unstable and the zonal flow impact will be much smaller compared to DIII-D results.

Summary

1. The zonal flow and zonal current are beat-driven generated by pump TAE with a twice linear growth rate.
2. Zonal current shows excellent agreement between simulation and theory, which gives rise to the "staircase-like" modification on safety factor profile.
3. For the strong EP-drive case, large zonal flow generation is due to the neoclassical polarization of EP and classical polarization of thermal ion (See Prof. Liu Chen's talk)
4. EP-PSZS exhibits hole-clump structures, correlated to TAE mode structure envelope, which weakens the EP drive.
5. ZF effects on EP nonlinearity slightly enhance the TAE saturation amplitude.
6. Bulk plasma nonlinearity dominates over zonal fields generation and TAE saturation.

Happy birthday to Professor Chen!